Evolution of the Electronic Structure in a Conjugated Polymer Series: Polyacetylene, Poly(*p*-phenylene), and Poly(*p*-phenylenevinylene)

M. Lögdlund* and W. R. Salaneck

Department of Physics, IFM, Linköping University, S-581 83 Linköping, Sweden

F. Meyers and J. L. Brédas

Service de Chimie des Matériaux Nouveaux, Université de Mons-Hainaut,
B-7000 Mons, Belgium

G. A. Arbuckle

Department of Chemistry, Rutgers University, Camden, New Jersey 08102

R. H. Friend

Cavendish Laboratory, Cambridge University, Cambridge CB3 0HE, U.K.

A. B. Holmes

University Chemical Laboratory, Lensfield Road, Cambridge CB2 1EW, U.K.

G. Froyer

IUT Sciences et Génie de Matériaux, Bâtiment ISITEM-La Chantrerie CP 3023,
44087 Nantes Cedex 03, France

Received March 1, 1993

ABSTRACT: Poly(*p*-phenylenevinylene) can be loosely viewed as a regular copolymer of polyacetylene and poly(*p*-phenylene). Here, the electronic structures of polyacetylene, poly(*p*-phenylene), and poly(*p*-phenylenevinylene) have been studied using ultraviolet photoelectron spectroscopy and quantum chemical calculations based upon the valence effective Hamiltonian method. Excellent agreement between theory and experiment allows for a detailed description of the evolution of the electronic structure in this polymer series.

Introduction

The discovery that polyacetylene can be doped to high conductivity[1] initiated a new research field which is still growing strongly. Initially, research focused on the metallic-like properties of these new quasi-1D metals, the so-called *conducting polymers*. Since then, attention has also been drawn to the unique properties of these materials in the *nonconducting* state, that is, of the conjugated polymers themselves. The fabrication of light emitting diodes (LED's)[2–5] and of field effect-transistors[6] based on conjugated polymers demonstrates important applications where these polymers are the main active components and are being used in the undoped (nonconducting) state. Additional interesting properties of conjugated polymers include remarkable nonlinear optical properties.[7,8]

It is well-known that polyacetylene (PA) can be doped to very high electrical conductivities[9,10] but that it is not particularly processible as a polymer material. Poly(*p*-phenylene) (PPP) is a thermally stable polymer but exhibits a more modest maximum electrical conductivity.[11] On the other hand, poly(*p*-phenylenevinylene) (PPV), the unit cell of which can be loosely considered to be a mixing of those of *trans*-PA and PPP, exhibits a desirable range of properties, including processibility. The chemical structures of the three polymers are shown in Figure 1. Note that *trans*-PA is quite unique in being a so-called degenerate ground-state system, which means that there are two equivalent geometrical structures in the ground state with the same total energy.[12] On the other hand, PPP and PPV are nondegenerate ground-state systems, where a single geometry of lowest total energy is found.

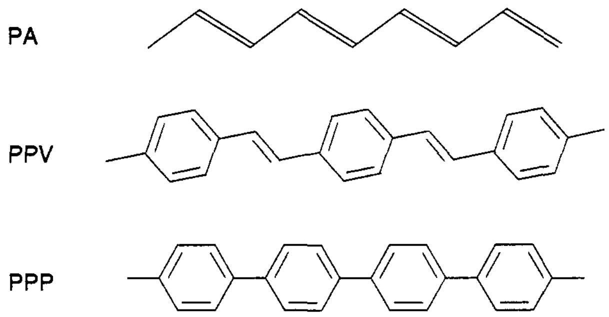

Figure 1. Molecular structures from top to bottom, of polyacetylene (PA), poly(*p*-phenylenevinylene) (PPV), and poly(*p*-phenylene) (PPP).

In this paper, we report the results of a detailed experimental study of the electronic structures of PA, PPP, and PPV using ultraviolet photoelectron spectroscopy (UPS). The evolution of the electronic structure in this polymer series is discussed through a comparison of the UPS valence electron spectra with the results of quantum chemical calculations based upon the valence effective Hamiltonian (VEH) method.[13,14] The good agreement between experiment and theory allows for a detailed discussion of the electronic structure characteristics of the polymers.

Experimental studies of the electronic structures of PA,[15–17] PPP,[18,19] and PPV[20–22] have been reported previously. It is not the purpose of this paper to provide an overview of these works; here, our goal is to investigate these three polymer materials as an intimately related polymer series: (i) to present improved UPS spectra; (ii) to analyze all the results with one common and well-established theoretical model; and (iii) to discuss the *evolution of the electronic structure within the polymer series*. The experimental valence bands of PA[15] and He I PPP,[23] which are used here, were recently reported in conference proceedings. In the case of PPV, new UPS spectra, exhibiting higher net energy resolution than those published previously, are presented.

Experimental Details

Free-standing films of *cis*-PA were prepared at the University of Pennsylvania and at Rutgers University by the standard Shirakawa method.[24] Free-standing films (30–50 μm thick) of *cis*-PA were shipped, under vacuum in sealed glass tubes, to the MAX Laboratory for Synchrotron Radiation in Lund. The samples were then transferred (quickly, but in air) into a Ultra high vacuum (UHV) spectrometer and heated to 160 °C for 30 min in order to convert to the *trans* form. Measurements were made using photon energies between 27 and 125 eV. The effects of photon energy dependent photoionization cross sections have been reported elsewhere.[15] Here, we have included the valence band recorded using photon energies of 27 and 50 eV only. The samples were thin enough that sample charging did not occur.

Ultrathin PPP films were deposited onto Cu substrates by electroreduction of 4,4′-dibromobiphenyl in the presence of a nickel complex catalyst,[25] at CNET,Lannion, France.

Thin films of PPV were prepared on metallized silicon substrates by spin-coating a solution of the tetrahydrothiophenium precursor polymer in methanol and converting to PPV by heating in vacuum for 10 h at 300 °C. The resulting samples were a few hundred ångströms in thickness. Conditions for the synthesis of the precursor polymers are discussed in ref 26. The PPV produced by this route has been extensively used for the fabrication of polymer LED's[2] and shows vibronic structure in form of shoulders in the absorption edge, as shown for example in ref 27. This structure is more pronounced than that seen in material prepared earlier[28] and is considered to indicate that there is better chain extension in the more recently-synthesized materials. However, modifications to the synthesis route can produce still better ordered material, with sharper vibrational features in the optical absorption.[29,30]

The samples of PPP and PPV were shipped to Linköping, sealed in proper ways. The samples were then inserted directly into a closed N_2 atmosphere in an "introduction chamber" of a specially designed and built photoelectron spectrometer. The films were then heated to 100 °C, in a base vacuum of about 10^{-10} Torr, in order to remove hydrocarbon contamination and any possible remaining solvent. Because of the surface sensitivity of UPS, this heating step is essential in order to obtain high-quality spectra. The effects of such heating (cleaning) procedures can be observed spectroscopically. UPS of PPV and PPP was carried out in Linköping, using monochromatized He I (21.2 eV) and He II (40.8 eV) photons. For the lowest binding energy C 2p derived bands, i.e., the π-bands, the cross section is higher for He I than for He II. The higher energy He II light provides the possibility of studying more of the inner-valence energy region.

Theoretical Calculations

The electronic structure calculations are based on the valence effective Hamiltonian (VEH) pseudopotential method, the parameters for which are determined by fitting to double-ζ-quality *ab initio* results on model molecules.[13,14] The applicability of the VEH model to the study of conjugated polymers is well established.[31–34] For a polymer chain, the output of a VEH calculation is a set of energy-*vs*-momentum curves, $E(\mathbf{k})$, the *band structure*. The density-of-valence-states (DOVS) curves, which are used to facilitate the interpretation of the UPS valence electron spectra, are directly computed in the standard way, by taking the inverse of the derivative of the energy-*vs*-momentum curves. In order to make a direct comparison between a calculated DOVS and an experimental solid-state UPS valence band spectrum, a standard three-step procedure is used. First, the DOVS the broadened by convolution with a Gaussian, whose full width at half-maximum is taken to be 0.7 eV; this is in order to simulate the experimental resolution as well as peak broadening due to solid state effects, i.e., interchain interactions and disorder effects. Second, a contraction along the energy axis is made, since the parameters used in VEH are based on Hartree–Fock calculations, which are known to exaggerate the total width of the valence band. The standard contraction factor of 1/1.3 has been used in this work. Third, a rigid shift along the energy axis is necessary, in order to align the calculated DOVS with the experimental UPS spectra. The shift is toward lower binding energy and allows one to take account of intermolecular relaxation effects in the solid, which are not included in the calculations (since these are performed on isolated chains). The energy shift is typically on the order of 1–2 eV.[35] The VEH model provides directly good estimates of the electron energy gap, E_g, and first ionization potential, I_p.

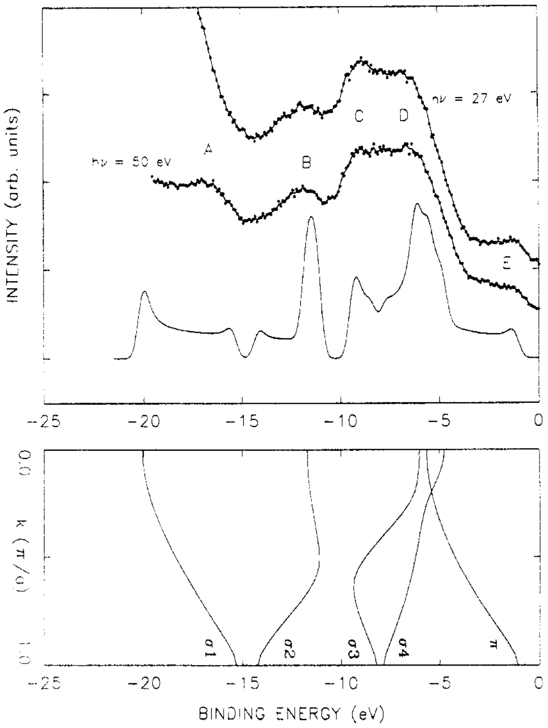

Figure 2. Valence band spectra of PA, recorded using synchrotron radiation at 27 eV, and 50-eV photon energy, and the corresponding VEH DOVS curves. The VEH band structure, at the same energy scale, is shown in the lower part of the figure.

The molecular geometries, used as input to the VEH calculations, are obtained using Hartree–Fock semiempirical Austin Model 1 (AM1) geometry optimization.[36] The calculations have been performed on oligomers of the different polymers, of which the central part is then used as input geometry to the VEH calculations. The AM1 method is known to yield reliable geometries for large organic molecules. In the case of PPP, however, torsion angles used are taken from experimental data, as discussed below.

Results and Discussion

The experimental UPS valence spectra, the convoluted DOVS derived from the VEH band structures, and the VEH band diagrams themselves are shown for (a) *trans*-PA in Figure 2, (b) PPV in Figure 3, and (c) PPP in Figure 4. The energy positions of the major and even minor peak structures in the UPS spectra for all three polymers are

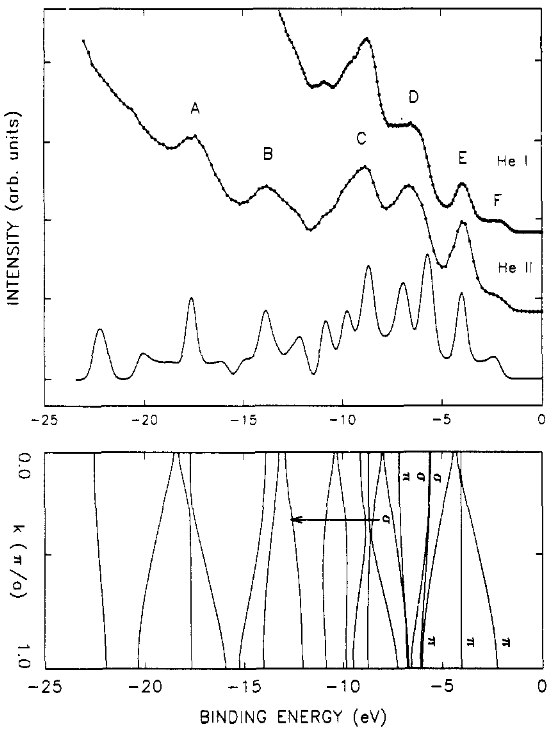

Figure 3. He I and He II valence band spectra of PPV and the corresponding VEH DOVS curves. The VEH band structure, at the same energy scale, is shown in the lower part of the figure.

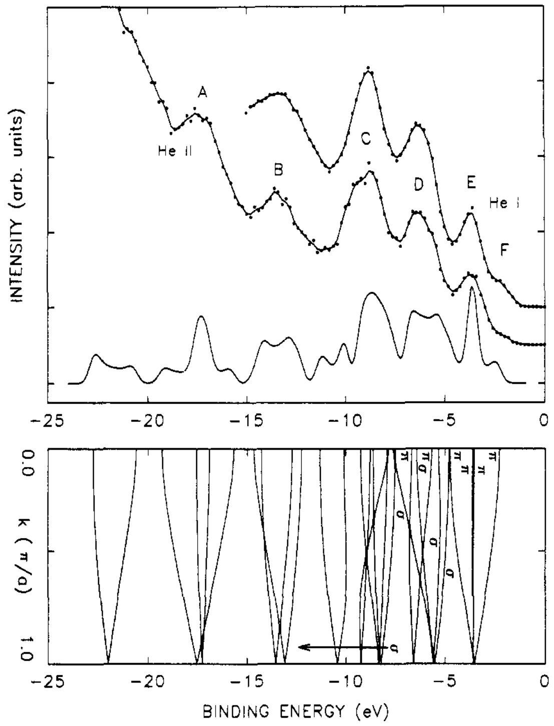

Figure 4. Valence band spectra of PPP, recorded with He I and He II radiation, and the corresponding VEH DOVS curves. In the lower part of the figure is shown the VEH band structure, at the same energy scale.

very well fit by the theoretical DOVS. The intensities, however, are in less good agreement, especially at higher binding energies. This is because photoionization cross-section effects have not been included in the calculations; these cross-section effects influence the higher binding energy peak intensities mostly. At typical UPS photon energies, the experimental photoionization cross section for C 2s derived orbitals, which dominate at higher binding energies, is about 5–10 times lower than the cross section for C 2p derived orbitals,[37] which dominate the spectra at low binding energies. Also, the spectra are affected by the secondary-electron distribution, producing a high background at higher binding energies. Especially in the He I spectra and for the spectrum of PA, taken with $h\nu = 27$ eV, a strong increasing background intensity, from about −15 eV and down in energy, can be seen. Taken together, these effects make it difficult to analyze the absolute intensities in the various UPS spectra.

(a) Polyacetylene. *trans*-PA has a planar zigzag configuration, with alternating single and double bonds of 1.44 and 1.36 Å.[38] However, the input geometry for the VEH calculations has been taken from AM1 geometry optimizations on an oligomer of *trans*-PA, in order to have the same procedure for all three polymers studied in this work. The differences are small and are not found to affect any of the results (the AM1-optimized bond lengths are 1.44 and 1.35 Å).

In Figure 2 are shown, from top to bottom, the following: (i) the experimental valence band of *trans*-PA recorded with photon energies of 27 and 50 eV; (ii) the DOVS convoluted from the VEH calculation; and (iii) the energy band diagram, from which the DOVS has been calculated. The energy scale is that which is determined experimentally, i.e., with respect to the Fermi level in the UPS spectra.

The electronic structure of *trans*-PA can be rationalized in the following manner.[14] In the absence of dimerization, i.e., with equal C—C and C═C bond lengths, polyacetylene would be a "regular polyene", and the unit cell would consist of a single (–CH–) group. At least within one-electron theory, there would exist three occupied valence bands, corresponding, in localized bond orbital terminology, to approximately a C–C σ-band, a C–H σ-band, and a π-band, the latter being derived from the remaining p_z atomic orbital on each C atom (the *z*-axis being perpendicular to the molecular plane). Since there would be one electron in each p_z atomic orbital on each C atom, the occupied π-band would be only half-filled and the electronic structure of the polymer would have a metallic character. Because of a Peierls transition (or, equivalently in molecular terminology, a Jahn–Teller distortion), the system is actually dimerized with alternating single and double carbon–carbon bonds. The unit cell in *trans*-PA contains two carbon atoms, corresponding to (–CH═CH–) units. In the unit cell with two C atoms, the width of the one-dimensional Brillouin zone is only half that for the case of the (hypothetical) regular polyene; therefore, each band of the regular polyene is split into two bands. In the dimerized unit cell, there are thus four occupied σ-bands and one occupied π-band. Due to the presence of dimerizations, there are energy gaps at the Brillouin zone edge, near −8 and −15 eV in Figure 2, where each pair of bands from the regular polyene structure is folded back to form the dimerized-chain band structure. The Peierls gap in the π-band, which occurs at the Brillouin zone edge, corresponds to the forbidden energy gap of approximately 1.5 eV in *trans*-PA. In addition, at the points where two σ-bands of like symmetry intend to cross, there is an avoided-band-crossing effect, as can be seen near −10 eV in Figure 2.

Peak A in the spectra corresponds to electrons from a band derived almost exclusively from C 2s atomic orbitals, i.e., the C–C backbone. Peak B is derived from the flat portion of the σ_2-band near the zone center. Peaks C and D correspond to electrons from the σ_2- and σ_3-bands derived from combinations of C–C and C–H bands at points in the Brillouin zone where there is a high density of states, i.e., at the zone center near −12 eV and at the zone edge near

Table I. A Comparison between the UPS and VEH Results

feature	binding energy (±0.1 eV)		
	He I	He II	VEH
A		-17.4	-17.6
B		-13.8, -12.4	-13.9, -12.2
C	-8.7	-8.8	-8.7
D	-7.5 to -6.0	-6.6	-7.0, -5.7
E	-4.0	-4.0	-4.0
F	-3.0 to -2.0	-2.4	-2.5

-8 eV. The broad peak E has its origin in the strongly dispersed π-band, which also contributes to peak D. The valence band edge corresponds to the highest portion of the occupied π-band, at the zone edge (at -2 eV in the calculated band structure of Figure 2).

As mentioned above, the σ-bands can loosely be referred to as C–C and C–H. In polyethylene, the upper bands are essentially C–H and the lower C–C. Because of the large dispersion in polyacetylene, however, this separation in energy does not occur. In polyacetylene, the upper σ-level (constituting the ionization potential for σ-electrons) is formed mainly from C $2p_y$ and H 1s atomic orbitals (the x-axis being the chain axis). This aspect is equivalent to what is obtained in saturated chains such as polyethylene and polysilane.[14]

(b) Poly(*p*-phenylenevinylene). Recent neutron-diffraction measurements on oriented PPV at room temperature have shown that the ring torsion angles, i.e., the twist of the phenyl rings out of the vinylene plane, are on the order of 7 ± 6°.[39] Such small torsion angles result in negligible effects on the calculated electronic band structure compared with that for the fully coplanar conformation. Therefore, PPV is taken to be planar in the VEH calculations used here. However, the freezing-out of these small ring torsions causes a red-shift in the band gap, which amounts to about 0.1 eV between room temperature and liquid-helium temperature.[30]

The DOVS of PPV, calculated from the VEH band structure, is compared with the experimental He I and He II spectra in Figure 3. The corresponding band structure is shown in the bottom part of the figure. The energy scale is fixed relative to the experimental Fermi level.

Peaks A–C originate from electrons in σ-bands. Peak D is built up from contributions from the four highest σ-bands, the lowest π-band, and a small portion from the relatively flat part of the second π-band. Peak E is derived from the next-highest π-band, which is extremely flat, since it corresponds to electronic levels fully localized on the bonds between ortho carbons within the phenyl rings. In general, a flat band results in a high-intensity peak in the DOVS, since there are many states per unit energy just at the flat band. There also are small contributions to peak E from the second and fourth π-bands. Finally, peak F is derived from the top part of the highest π-band. The larger dispersion of the top π-band results in lower intensity in the UPS data. The resolution of the peaks and shoulders in the UPS spectra, particularly in the region of the π-bands, is considerably improved over that of earlier measurements. This may be due to the overall improvement of the samples, i.e., only trace amounts of oxygen, and in particular the improved conformational order in the polymer. The calculated and measured binding energies are in very good agreement for PPV, as illustrated in Table I.

(c) Poly(*p*-phenylene). A torsion angle of 22.7° between two successive benzene rings is used in the calculations, following crystallographic data on oligomers of PPP in the solid state.[40–42] The finite torsion angle is the net result of the steric repulsion between the hydrogen atoms in the ortho positions of neighboring phenyl rings, which induce a nonplanar structure, and the effects of conjugation and crystal packing, which favor a planar structure. Because of the finite torsion angle, the unit cell contains two benzene rings, thus increasing the number of occupied π-bands from 3 to 6, compared with a totally flat PPP, for which there would be only one ring in the unit cell.

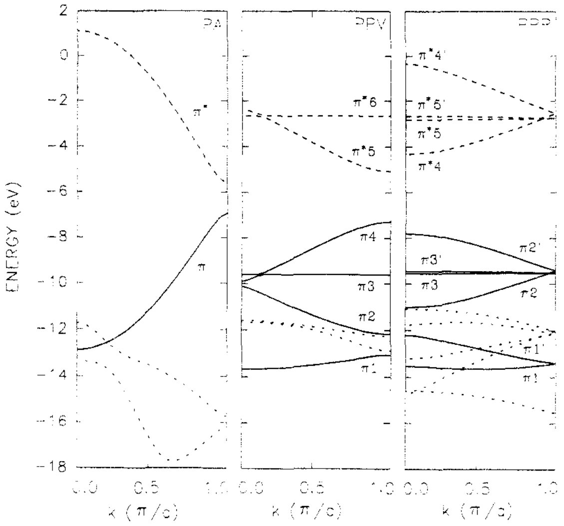

Figure 5. Upper part of the VEH band structures for PA, to the left, PPV, in the middle, PPP, to the right. Included are some of the unoccupied bands (long dashed lines), all of the occupied π-bands (solid line), and some of the occupied σ-bands (short dashed lines).

In Figure 4 are shown, from top to bottom, the experimental valence band of PPP for He I and He II and the DOVS convoluted from the VEH calculation. The band diagram, from which the DOVS is calculated, is shown in the bottom part of Figure 4. The energy scale is relative to the experimental Fermi level.

Peaks A–C correspond to electrons originating from σ-bands. Peak D has contributions from several bands, the main contributions coming from the highest σ-bands and the three lowest lying π-bands. Peak E corresponds mainly to electrons in the two, extremely flat, occupied π-bands. However, the other two highest occupied π-bands provide also some contributions to peak E. Finally, peak F corresponds to electrons in the highest occupied π-band.

(d) Evolution of the Electronic Structure. In Figure 5 are shown the upper parts of the band structures for PA, PPV, and PPP. Included are some of the unoccupied bands (long dashed lines), all occupied π-bands (solid lines), and some of the occupied σ-bands (short dashed lines). The energy scale in Figure 5 is relative to the theoretical vacuum level, and no contractions have been made.

On the left in Figure 5, are shown the π^*, π, and the two highest occupied σ-bands for PA. The only occupied π-band is very dispersed, with a bandwidth of about 6 eV. The calculated bandwidth of the lowest unoccupied π-band, π^*, is about 6.7 eV. The VEH calculation yields a band gap of E_g = 1.34 eV. Optical absorption on *trans*-PA has a maximum (first absorption peak) at 1.8 eV.[43]

To the right in Figure 5 are shown the four lowest π^*, the six occupied π-bands, and the five highest occupied σ-bands of PPP. As discussed above, the presence of a finite torsion angle between two successive benzene rings decreases the size of the Brillouin zone such that the number of bands in the system increases from 3 to 6 occupied π-bands. Taking the glide plane symmetry along the chain axis into account, which causes the bands to be degenerate two by two at the end of the Brillouin zone,

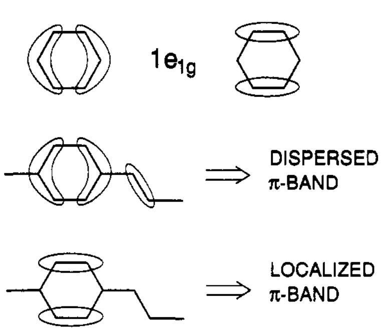

Figure 6. Molecular origin of the dispersed and localized π-bands in PPV and PPP.

one can identify three occupied π-bands. The occupied π-bands for PPP are related to the molecular orbitals in benzene as follows. Bands π2–π2′ and π3–π3′ are built up out of the doubly degenerate $1e_{1g}$ benzene molecular orbital. The origin of the separation into dispersed bands and nondispersed (localized) bands is illustrated in Figure 6. The π3–π3′ levels are localized to the ortho carbons in the benzene rings; i.e., the interaction is negligibly small between neighboring rings, which results in very flat bands. The wavefunction of the $1e_{1g}$ state of the benzene moiety that has a nonzero intensity at the carbon atoms where the neighboring benzene rings are bound interacts with those of the neighboring benzenes, leading to the generation of the dispersed π-band π2–π2′ (with a band width of about 3.2 eV). Finally, the π1–π1′ levels are related to the $1a_{2u}$ orbital in benzene, which is evenly spread out over the ring; there is correspondingly interaction between rings, resulting in a total bandwidth of about 1.3 eV.

The band gap in PPP is calculated to be $E_g = 3.29$ eV. The maximum absorbance of the first peak in the optical absorption of PPP varies depending on the sample preparation method, with values ranging from 3.2,[25] 3.34,[44] 3.4,[45] to 3.65 eV;[46] these variations may also correspond to (average) departures from the small torsion angle distribution mentioned above. A larger torsion angle leads to a larger electronic band gap, resulting in a larger optical absorption edge energy.

Finally, in the middle of Figure 5 are shown the two lowest π*, the four occupied π, and the two highest occupied σ-bands of PPV. The unit cell of PPV consists of a styrene unit. Upon attaching a vinylene group to a benzene molecule, the doubly degenerate outermost π-orbitals split into two orbitals as a result of lifting the degeneracy.[47–49] As in the case of PPP, the π3 band is localized on the ortho carbons, i.e., it consists of localized states. The wavefunction which has a nonzero intensity at the para carbon atoms (where the neighboring vinylene groups are bound) interacts with the π-state of the vinylene group, as illustrated in Figure 6, leading to the generation of the dispersed π-bands π2 and π4. The top of the π4 band has almost equal contributions from the vinylene and the phenylene groups. Due to the lack of symmetry within the unit cell, an avoided band crossing occurs between the π3 and π4 bands near the zone center. The difference between the top of band π4 and the flat band π3 is about 2.3 eV. The flat band π3 appears only about 0.3 eV above what would have been the bottom part of the wide π4 band in the absence of an avoided crossing. The bandwidth of π2 is about 2.0 eV, i.e., almost the same degree of delocalization as π4. Finally, the bandwidth of π1 is about 0.6 eV. This band is, as in the case of π1–π1′ in PPP, related to the $1a_{2u}$ orbital in benzene. The dispersion, however, has decreased in PPV, since the only occupied π-orbital of the vinylene group only interacts weakly with the $1a_{2u}$ state of benzene, from which the π1–π1′-band in PPP is derived.

For PPV, the VEH calculation yields a band gap of $E_g = 2.27$ eV. Optical absorption spectra of well-oriented PPV samples exhibit the maximum of the first absorption peak at 2.5 eV.[30]

Summary

The evolution of the electronic structure within a series of conjugated polymers, polyacetylene, poly(*p*-phenylene), and poly(*p*-phenylenevinylene), has been studied by means of ultraviolet photoelectron spectroscopy (UPS) and the results of VEH quantum chemcial calculations. The good agreement between theory and experiment enables a detailed description of the evolution of the valence band structure. In particular, the VEH results agree with the experimental total bandwiths, the detailed structures in the spectra. The origin of the important π-bands has been illustrated through a discussion of the nature of the degenerate $1e_{1g}$ orbital of benzene. These results represent the basis for understanding the electronic nature of the band structure evolution in conjugated polymers based on phenylene and vinylene groups.

Acknowledgment. The authors acknowledge the help of S. C. Graham, A. B. Brown, and P. L. Burn, in the preparation of the PPV samples. The Linköping–Mons and Mons–Cambridge collaborations are supported by the Commission of the European Community, within the SCIENCE programme (Project 0661 POLYSURF) and the BRITE/EURAM programme (Project 0148 NAPOLEO), respectively. Research on conjugated polymers in Linköping is supported in general by grants from the Swedish Natural Science Research Council (NFR), the Swedish National Technical Research Board (TFR), the Swedish National Board for Industrial and Technical Development (NuTek), and Neste Corp., Finland. The work in Mons is partly supported by the Belgian Government "Pôle d'Attraction en Chimie Supramoléculaire et Catalyse", the SPPS "Programme d'Impulsion en Technologie de l'Information (Contract IT/SC/22)", and FNRS.

References and Notes

(1) Chiang, C. K.; Fincher, C. R.; Park, Y. W.; Heeger, A. J.; Shirakawa, H.; Louis, E. J.; Gau, S. C.; MacDiarmid, A. G. *Phys. Rev. Lett.* **1977**, *39*, 1098.
(2) Burroughes, J. H.; Bradley, D. D. C.; Brown, A. R.; Marks, R. N.; Mackay, K.; Friend, R. H.; Burn, P. L.; Holmes, A. B. *Nature* **1990**, *347*, 539.
(3) Burn, P. L.; Holmes, A. B.; Kraft, A.; Bradley, D. D. C.; Brown, A. R.; Friend, R. H. *Nature* **1992**, *356*, 47.
(4) Braun, D.; Heeger, A. J. *Appl. Phys. Lett.* **1991**, *58*, 1982.
(5) Gustafsson, G.; Cao, Y.; Treacy, G. M.; Klavetter, F.; Colaneri, N.; Heeger, A. J. *Nature* **1992**, *357*, 477.
(6) Garnier, F.; Horowitz, G.; Peng, X.; Fichou, D. *Adv. Mater.* **1990**, *2*, 592.
(7) Heeger, A. J.; Orenstein, J.; Ulrich, D. R., Eds. *Nonlinear Optical Properties of Polymers*; Materials Research Society: Pittsburgh, PA, 1988.
(8) Brédas, J. L., Chance, R. R., Eds. *Conjugated Polymeric Materials: Opportunities in Electronics, Optoelectronics and Molecular Electronics*; Kluwer: Dordrecht, The Netherlands, 1990.
(9) Skotheim, T. A., Ed. *Handbook of Conducting Polymers*; Dekker: New York, 1986. Brédas, J. L., Silbey, R., Eds. *Conjugated Polymers: The Novel Science and Technology of Highly Conducting and Nonlinear Optically Active Materials*; Kluwer: Dordrecht, The Netherlands, 1991.
(10) Naarmann, H.; Theophilou, N. *Synth. Met.* **1987**, *22*, 1.
(11) Ivory, D. M.; Miller, G. G.; Sowa, J. M.; Shacklette, L. W.; Chance, R. R.; Baughman, R. H. *J. Chem. Phys.* **1979**, *71*, 1506.
(12) Brédas, J. L.; Street, G. B. *Acc. Chem. Res.* **1985**, *18*, 309.
(13) Brédas, J. L.; Chance, R. R.; Silbey, R.; Nicolas, G.; Durand, Ph. *J. Chem. Phys.* **1981**, *75*, 255.

(14) André, J. M.; Delhalle, J.; Brédas, J. L. *Quantum Chemistry Aided Design of Organic Polymers*; World Scientific: Singapore, 1991.

(15) Rasmusson, J.; Stafström, S.; Lõgdlund, M.; Salaneck, W. R.; Karlsson, U.; Swanson, D. B.; MacDiarmid, A. G.; Arbuckle, G. A. *Synth. Met.* **1991**, *41–43*, 1365.

(16) Salaneck, W. R. In *Handbook of Conducting Polymers*; Skotheim, T. A., Ed.; Dekker: New York, 1986; Chapter 37.

(17) Kamiya, K.; Inokuchi, H.; Oku, M.; Hasegawa, S.; Tanaka, C.; Tanaka, J.; Seki, K. *Synth. Met.* **1991**, *41–43*, 155.

(18) Seki, K.; Karlsson, U. O.; Englehardt, R.; Koch, E.-E.; Schmidt, W. *Chem. Phys.* **1984**, *91*, 459.

(19) Riga, J.; Pireaux, J. J.; Boutique, J. P.; Caudano, R.; Verbist, J. J.; Gobillon, Y. *Synth. Met.* **1981**, *4*, 99.

(20) Obrzut, J.; Obruzt, M. J.; Karasz, F. E. *Synth. Met.* **1989**, *29*, E109.

(21) Seki, K.; Asada, S.; Mori, T.; Inokuchi, H.; Murase, I.; Ohnishi, T.; Noguchi, T. *Solid State Commun.* **1990**, *74*, 677.

(22) Sato, N.; Lõgdlund, M.; Lazzaroni, R.; Salaneck, W. R.; Brédas, J. L.; Bradley, D. D. C.; Friend, R. H.; Ziemelis, K. E. *Chem. Phys.* **1992**, *160*, 299.

(23) Lõglund, M.; Salaneck, W. R.; Stafström, S.; Bradley, D. D. C.; Friend, R. H. Ziemelis, K. E.; Froyer, G.; Swanson, D. B.; MacDiarmid, A. G.; Arbuckle, G. A.; Lazzaroni, R.; Meyers, F.; Brédas, J. L. *Synth. Met.* **1991**, *41–43*, 1315.

(24) Shirakawa, H.; Ikeda, S. *Synth. Met.* **1979/1980**, *1*, 175.

(25) Fauvarque, J.-F.; Petit, M.-A.; Digua, A.; Froyer, G. *Makromol. Chem.* **1987**, *188*, 1833.

(26) Burn, P. L.; Bradley, D. D. C.; Friend, R. H.; Halliday, D. A.; Holmes, A. B.; Jackson, R. W.; Kraft, A. M. *J. Chem. Soc., Perkin Trans. 1* **1992**, 3225.

(27) Friend, R. H.; Bradley, D. D. C.; Brown, A. R.; Graham, S. C.; Halliday, D. A.; Burn, P. L.; Kraft, A.; Holmes, A. B. *Mol. Cryst. Liq. Cryst.* **1992**, *216*, 33.

(28) Colaneri, N. F.; Bradley, D. D. C.; Friend, R. H.; Burn, P. L.; Holmes, A. B.; Spangler, C. W. *Phys. Rev.B.* **1990**, *42*, 11671.

(29) Burn, P. L.; Bradley, D. D. C.; Brown, A. R.; Friend, R. H.; Halliday, D. A.; Holmes, A. B.; Kraft, A.; Martens, J. H. F. *Springer Ser. Solid-State Sci.* **1992**, *107*, 293.

(30) Halliday, D. A.; burn, P. L.; Bradley, D. D. C.; Friend, R. H.; Gelsen, O.; Holmes, A. B.; Kraft, A.; Martens, J. H. F.; Pichler, K. *Adv. Mater.* **1993**, *5*, 40.

(31) Orti, E.; Brédas, J. L. *J. Chem. Phys.* **1988**, *89*, 1009.

(32) Salaneck, W. R. *CRC Crit. Rev. Solid State Mater. Sci.* **1985**, *12*, 267.

(33) Brédas, J. L.; Salaneck, W. R. *J. Chem. Phys.* **1986**, *85*, 2219.

(34) Brédas, J. L.; Chance, R. R.; Silbey, R.; Nicolas, G.; Durand, Ph. *J. Chem. Phys.* 1981, *77*, 371.

(35) Sato, N.; Seki, K.; Inokuchi, H. *J. Chem. Soc., Faraday Trans. 2* **1981**, *77*, 1621.

(36) Dewar, M. J. S.; Zoebish, E. G.; Healy, R. F.; Stewart, J. J. P. *J. Am. Chem. Soc.* **1985**, *107*, 3902.

(37) Yeh, J. J.; Lindau, I. *At. Data Nucl. Data Tables* **1985**, *32*, 1.

(38) Yannoni, C. S.; Clarke, T. C. *Phys. Rev. Lett.* **1983**, *51*, 1191.

(39) Mao, G.; Fisher, J. E.; Karasz, F. E.; Winokur, M. J. *Phys. Rev. B*, in press.

(40) Delugeard, Y.; Desuche, J.; Baudour, J. L. *Acta Crystallogr. Sect. B.* **1976**, *32*, 702.

(41) Baudour, J. L.; Cailleau, H.; Yelon, W. B. *Acta Crystallogr. Sect. B* **1977**, *33*, 1773.

(42) Baudour, J. L.; Delugeard, Y.; Rivet, P. *Acta Crystallogr. Sect. B* **1978**, *34*, 625.

(43) Chung, T.-C.; Moraes, F.; Flood, J. D.; Heeger, A. J. *Phys. Rev. B.* **1984**, *29*, 2341.

(44) Shacklette, L. W.; Eckhardt, H.; Chance, R. R.; Miller, G. G.; Ivory, D. M.; Baughman, R. H. *J. Chem. Phys.* **1980**, *73*, 4098.

(45) Satoh, M.; Kaneto, K.; Yoshino, K. *J. Chem. Soc., Chem. Commun.* **1985**, 1629.

(46) Leising, G.; Pichler, K.; Stelzer, F. *Electronic Properties of Conjugated Polymers III*; Kuzmany, H., Mehring, M., Roth, S., Eds.; Springer-Verlag: Heidelberg, 1989; p 100.

(47) Rabalais, J. W.; Colton, R. J. *J. Electron Spectrosc. Relat. Phenom.* **1972/1973**, *1*, 83.

(48) Maier, J. P.; Turner, D. W. *J. Chem. Soc., Faraday Trans. 2* **1973**, *69*, 196.

(49) Johnstone, R. A. W.; Mellon, F. A. *J. Chem. Soc., Faraday Trans. 2* **1973**, *69*, 1155.